Scripta Materialia xxx (2015) xxx–xxx

Contents lists available at ScienceDirect

Scripta Materialia

journal homepage: www.elsevier.com/locate/smm

Slip nucleation in single crystal FeNiCoCrMn high entropy alloy

L. Patriarca [a], A. Ojha [a], H. Sehitoglu [a,*], Y.I. Chumlyakov [b]

[a] Department of Mechanical Science and Engineering, University of Illinois at Urbana-Champaign, 1206 W. Green St., Urbana, IL 61801, USA
[b] Siberian Physical-Technical Institute at Tomsk State University, Tomsk 634050, Russia

ARTICLE INFO

Article history:
Received 12 August 2015
Accepted 6 September 2015
Available online xxxx

Keywords:
High entropy alloy
Slip
X-ray diffraction
Digital image correlation
Peierls stress. Critical resolved shear stress

ABSTRACT

We present an experimental and theoretical study of slip nucleation in high entropy FeNiCoCrMn alloy which possesses superb mechanical properties. Uniaxial compression experiments were conducted on the $[5\bar{9}1]$ oriented single crystals. The single crystals permit evaluation of critical resolved shear stress (CRSS), and using Digital Image Correlation strain measurements it is possible to track the slip nucleation precisely. The experimental value of 175 MPa for CRSS is in excellent agreement with 178 MPa obtained utilizing an advanced atomistic-modified Peierls–Nabarro modeling formalism. This close agreement demonstrates the efficacy of our methodology and has implications in design of new high entropy alloys.

1. Introduction

Engineering structures and components can experience extreme loading conditions, therefore the development of new materials with exceptional mechanical properties is of significant importance. The recently proposed high entropy alloys with equal atomic mass of multi-component elements hold considerable promise and provide a potential breakthrough where high strength and high toughness may coexist [1,2]. The key to engineer these alloys is to exploit the solid solution hardening that derives from the choice of the elements for strengthening and, alongside, to obtain a single phase alloy which promotes high toughness. In this direction, as already suggested in recent works [3,4], the FeNiCoCrMn alloy represents one of the most promising high entropy alloys. As discussed in the aforementioned works, in the early stages of FeNiCoCrMn deformation slip represents the main deformation mechanism. It is thus of fundamental importance to (i) precisely determine the stress required to nucleate slip, and (ii) accurately predict this critical resolved shear stress (CRSS) with theory and simulation without using empirical constants. Previous treatments focused on experiments on polycrystalline alloys. In this work, we focus on single crystals because they allow precise determination of CRSS for slip based on the applied stress through the Schmid factor. We successfully grew single crystals of this alloy for the first time which is an important undertaking in pursuit of better understanding of the mechanical response. In particular, we deform $[5\bar{9}1]$ oriented crystals, a predominantly single slip orientation, and determine the CRSS experimentally.

Recent experiments have been conducted to study the temperature dependence on the yield strength of FeNiCoCrMn [3–6]. It is found that the ultimate tensile strength and the uniform elongation to fracture in these alloys increase with decreasing temperature. Slip is considered the main deformation mechanism even at low temperatures. However, since most of the previous experiments are conducted on polycrystalline samples, it is difficult to determine CRSS, a fundamental quantity, because the stress state at the grain level is not known [7]. In the current work, we use single crystals of FeNiCoCrMn where the stress state is completely defined as stated above, and the CRSS can be established. We are utilizing high resolution digital image correlation (DIC) methodology developed in our early work [8,9] to accurately establish local strain development due to onset of slip. Similar to the fcc metals, slip occurs on {111}<110> system in FeNiCoCrMn with Burgers vector of magnitude $|b| = a_0/\sqrt{2}$, where a_0 is the lattice constant. We choose the $[5\bar{9}1]$ crystal orientation such that the {111}<110> slip system with the highest Schmid factor nucleates providing a way to precisely pinpoint the CRSS. With the choice of single crystal, the role of other defects such as grain boundaries is removed, and an intrinsic measure of CRSS for slip is obtained. The CRSS is an important parameter in crystal plasticity, dislocation dynamics or other continuum mechanics treatments of stress–strain response. This represents a fundamental step in multiscaling.

Concurrently, we undertake atomistic calculations to obtain the lattice constant a_0 and the important energy terms, γ_{us} (the unstable stacking fault energy) and γ_{isf} (the intrinsic stacking fault energy) associated with the generalized stacking fault energy (GSFE) curve. The GSFE curve represents the free energy differences between a crystal fault and the bulk lattice with various degrees of shear displacements

* Corresponding author. Tel.: +1 217 333 4112; fax: +1 217 244 6534.
E-mail address: huseyin@illinois.edu (H. Sehitoglu).

http://dx.doi.org/10.1016/j.scriptamat.2015.09.009
1359-6462/

[10]. The term γ_{us} represents the fault energy per unit area required to nucleate a slip, and γ_{isf} is equivalent to the differential of the hcp and fcc free energy per unit area. By utilizing the well-developed modified Peierls–Nabarro (PN) formalism for cubic metals [11–16], we then calculate the CRSS theoretically disclosing very close agreement with the experimentally observed value.

2. Experiments

Single crystals of the equiatomic FeNiCoCrMn high entropy alloy were grown using the Bridgman technique in a He atmosphere utilizing high purity single element pieces. Single crystal ingots were homogenized at 1200 °C for 24 h in vacuum and successively quenched. Compression specimens were sectioned into 3.8 mm × 3.8 mm × 8 mm using electro-discharged machining with the loading axis along the [5$\bar{9}$ 1] crystallographic direction. The single crystal compression specimens were successively solution-treated at 1100 °C for 1 h in air and quenched in oil. The crystal orientations of the specimens in three directions and the lattice parameters were determined by a Philips Xpert 2 X-ray diffractometer. The chemical composition was checked on one solution-treated sample by means of an ICP-MS PerkinElmer instrument providing the atomistic percentages Fe = 21.64%, Ni = 19.09%, Co = 21.47%, Cr = 18.35%, and Mn = 19.45%.

The experiments in compression were conducted on a MTS servo hydraulic load frame in displacement control at an average strain rate of 10^{-4} s^{-1}. A fine speckle pattern adapted for DIC correlation was deposited on one surface of the specimens. The images suited for DIC strain measurements were captured by means of an IMI model IMB-202 FT CCD camera (1600 × 1200 pixels) with a Navitar optical lens. Two different image acquisition techniques were adopted for the room temperature (293 K) and low temperature (77 K) experiments. At 293 K, the images were captured in-situ every 2 s during the loading and unloading for a region of 4 mm × 3 mm of the specimen surface. The local strains were successively obtained after correlation of the images. Using this technique, we precisely pinpointed the stress required to nucleate slip at 293 K as the local strain measurements are performed real-time. No extensometer was required as the nominal axial strain for constructing the stress–strain curve was obtained averaging the strain fields over the entire DIC region. For the experiment at 77 K in-situ DIC was not available as the specimen is constantly immersed in liquid nitrogen in order to maintain the low temperature during the experiment. In order to overcome this problem, we initially tested one specimen using an extensometer in order to construct the stress–strain curve at 77 K. Successively, on a virgin specimen, we performed the DIC strain measurements at zero load at 293 K, following incremental stress steps at 77 K. Three images of the entire lateral specimen surface were captured at RT before loading. Successively, the specimen was cooled at 77 K, and after temperature stabilization a small loading step was performed in stress–control. The specimen was successively dried and three images at RT were captured. The correlation provides the residual strain following the performed load step. Slip onset is then determined following the appearance of residual strains after a specific load step performed at the maximum stress of σ_{i+1}. As the increment of stress between the load steps was chosen to be 10 MPa, we defined the stress required to nucleate slip as $(\sigma_i + \sigma_{i+1})/2 \pm 5$ MPa. This procedure of slip nucleation stress determination for 77 K experiment is novel.

3. Experimental results

The stress–strain curve obtained at 293 K is reported in Fig. 1. In the top-right of Fig. 1 we provide the inverse pole figure calculated from X-ray data representing the [5$\bar{9}$1] crystal orientation of the specimens along the load direction. Contour plots of the real time in-situ DIC strain fields are reported in the insets from 1 to 4. Inset marked 1 shows the strain field of the analyzed region captured before slip onset. Inset marked 2 shows the appearance of strain localizations at σ = 140 MPa which indicate slip onset. With increasing the applied deformation, the regions displaying early slip show one primary [01$\bar{1}$]($\bar{1}$11) slip system (Schmid factor 0.50) and one secondary [0$\bar{1}\bar{1}$](1$\bar{1}$1) slip system (Schmid factor 0.44). Inset marked 5 shows the strain field captured for the entire specimen side after unloading. High strain localizations (>10%) were measured along the primary slip system, while large areas of the specimen remain undeformed.

Fig. 2 illustrates the results following the experimental procedure aimed to capture slip onset at 77 K. Only the main strain measurements

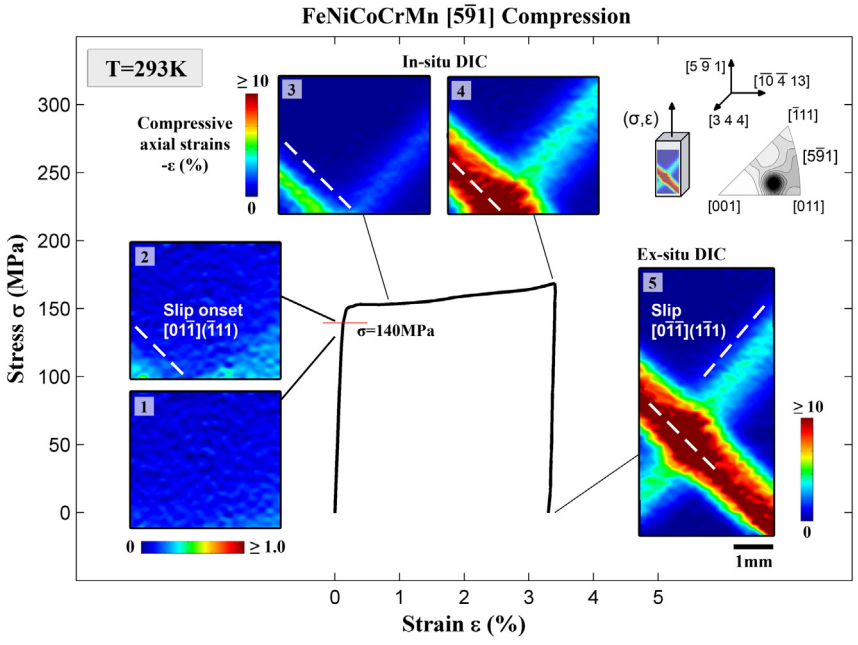

Fig. 1. Stress–strain behavior of the [5$\bar{9}$1] orientation tested in compression at room temperature. Real time in-situ DIC strain measurements (insets 1 to 4) show the onset of slip at the axial stress of σ = 140 MPa. One primary slip system is active during deformation, while a secondary slip system is also active. Inset marked 5 shows the residual strain field upon unloading.

Please cite this article as: L. Patriarca, et al., Slip nucleation in single crystal FeNiCoCrMn high entropy alloy, Scripta Materialia (2015), http://dx.doi.org/10.1016/j.scriptamat.2015.09.009

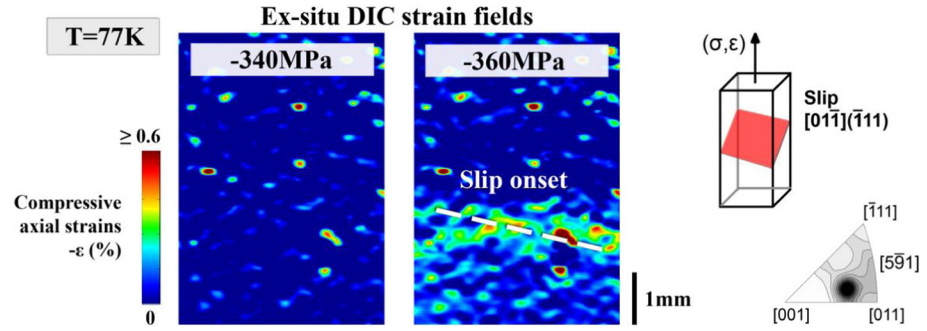

Fig. 2. Ex-situ DIC strain fields captured following loading the [5$\bar{9}$1] orientation in compression at T = 77 K. The images for DIC were captured after loading/unloading at different maximum compressive stresses (the most important ones reported are 340 MPa and 360 MPa). Slip is shown to be active after the application of a compressive stress of 360 MPa.

are reported for the sake of brevity. Two strain plots are shown representing the strain field after loading/unloading the specimen at a maximum compressive stress of 340 MPa and 360 MPa at 77 K. The first strain field (340 MPa) indicates that no slip was active following the first stress cycle at 340 MPa; we then conclude that at 77 K, a compressive stress of 340 MPa is not sufficient to activate slip. The second strain field displays strain localization along the dashed line which indicates that following the load step at 360 MPa some irrecoverable process occurred. According to the stress levels tested we then established the axial stress required to slip initiation as $\sigma = (350 \pm 10)$ MPa. Slip has been determined to be the dominant deformation mechanism even at 77 K. Twinning is not expected for this orientation as the Schmid factor for the most favorable twin system [12$\bar{1}$](1$\bar{1}$1) is lower than 0.40.

In Fig. 3 we summarized and compared the stress–strain curves for the compressive experiments carried out at 293 K and at 77 K for the present [5$\bar{9}$1] orientation. Using the Schmid law, we calculated the CRSS and obtained $\tau_{77K} = 175$ MPa and $\tau_{293K} = 70$ MPa at 77 K and 293 K respectively. The elastic moduli are $E_{77K} = 206$ GPa and $E_{293K} = 127$ GPa. In Fig. 3 we also report the X-ray diffraction data obtained on the single crystal specimen. The peak shown comes from the reflection of the (111) plane. We calculated the lattice parameter to be 3.585 Å.

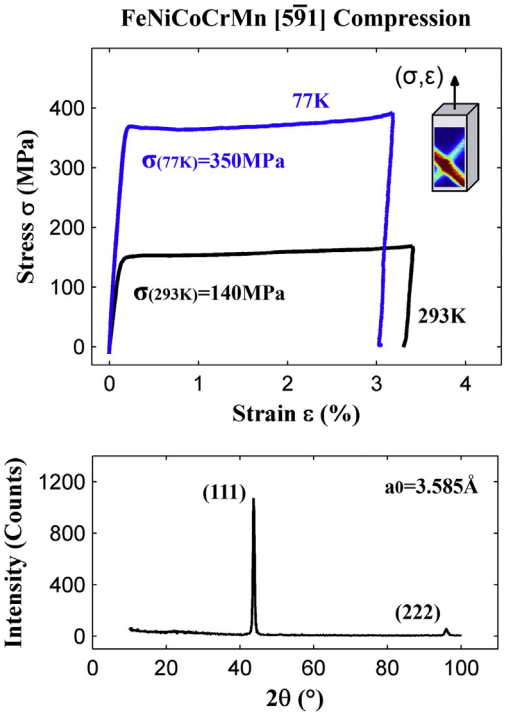

Fig. 3. Comparison of the stress–strain behaviors of the [5$\bar{9}$1] orientation tested in compression at T = 293 K and T = 77 K. The critical resolved shear stresses were determined according the activation of the slip system [01$\bar{1}$](1$\bar{1}$1) which has SF = 0.5 and using the axial stresses determined by DIC strain measurements.

4. Modeling of critical resolved shear stress for slip

Using the first principles density functional theory (DFT) calculations, we obtained the equilibrium lattice constant of FeNiCoCrMn as $a_0 = 3.59$ Å which is in close agreement with experiments, and this is the starting point for the simulations. The DFT calculations were performed utilizing the Vienna ab initio Simulation Package (VASP) [17,18] with the Projector Augmented Wave (PAW) method and the Generalized Gradient Approximation (GGA) [19,20]. To determine the slip nucleation stress, the unstable stacking fault energy (γ_{us}) and the intrinsic stacking fault energy (γ_{isf}) values associated with the GSFE curve for {111}<110> slip system were theoretically determined for the first time, as shown in Table 1. In order to address potential solute segregation effects [21–23] near the fault, it is important to check systematically the role of solute positions on the intrinsic stacking fault energy. In the present case, after many simulations, we noted that the presence of Co atoms are favored near the fault reducing the intrinsic stacking fault energy by almost 55% (lowered from 38 mJm^{-2} to 17 mJm^{-2}) when compared to the presence of Co positions away from the fault. Therefore, the stacking fault energies reported in Table 1 correctly represent the lowest energy values possible for the {111}<110> slip system. A relaxation scheme utilized in our previous work (atoms are allowed to adjust their positions normal to the fault plane [24]) ensured correct energy values as well. We note that without accounting for the solute segregation effects and implementing the relaxation scheme, the results would be in error. The GSFE landscape also allows us to derive the {110}<111> shear modulus using the equation $G = 2\pi\frac{\partial\gamma}{\partial u}|_{max}$ where $\frac{\partial\gamma}{\partial u}|_{max}$ is the maximum slope of the GSFE curve. Using this well-established formulation, the {111}<110> shear modulus (G) is obtained to be 84 GPa. We then utilized the 'modified' Peierls–Nabarro equation for cubic metals from our early studies [16,25–27] noting the appearance of the lattice parameter a_0, γ_{us} and γ_{isf} terms in the equation. Subsequently, the slip stress for FeNiCoCrMn was obtained as 178 MPa using modified PN stress equation $\tau = \frac{1}{b}\max\{\frac{dE_{misfit}}{du}\}$ as reported in Table 2. It is important to note that the misfit energy term in PN equation is dependent on a_0, γ_{us}, and γ_{isf}, and we obtained these terms theoretically in the present analysis. For complete description of the energy terms, and the PN formalism, please see Ref [11–13,15,16]. In addition, we also obtained the twinning stress for this alloy as 208 MPa using the methodology proposed in our early work (Wang-Sehitoglu [15]).

According to the experimental results shown in Fig. 3, the dependence of the CRSS on the temperature is striking. The CRSS at room

Please cite this article as: L. Patriarca, et al., Slip nucleation in single crystal FeNiCoCrMn high entropy alloy, Scripta Materialia (2015), http://dx.doi.org/10.1016/j.scriptamat.2015.09.009

Table 1
The lattice constant a0, {111}b110N shear modulus, the unstable and intrinsic stacking fault energies (γus and γisf) in mJ-m−2 for FeNiCoCrMn obtained in the present study. The experimental value for γisf is also given.

Material	a_0 (Å) (this study)	Shear modulus $G_{\{111\}<110>}$ (GPa, this study)	γ_{us} (mJm^{-2})	γ_{isf} (mJm^{-2})	γ_{isf} (mJm^{-2})
			Simulation (this study)		Experiment [28]
FeNiCoCrMn	3.59	84	192	17	20-25

Table 2
Critical resolved shear stress (CRSS) for slip in FeNiCoCrMn obtained experimentally in the present study. The stress level obtained based on the modified PN formalism at 0 K is also given.

Material	Temperature (K)	Critical resolved shear stress for slip τ (MPa)	
		Experiment (this study)	Theory[a]
FeNiCoCrMn	77	175 ± 5	178

[a] Based on Peierls–Nabarro equation, $\tau = \frac{1}{b}\max\{\frac{dE_{misfit}}{du}\}$.

temperature is 70 MPa while that at 77 K is 175 MPa, an increase in the stress by more than two-fold with decrease in temperature. Further simulations and derivation of the CRSS using PN formalism showed that the CRSS at low temperature is 178 MPa (see Table 2). It is suggested that the temperature dependence on the yield strength in these alloys is dictated by the Peierls stress similar to the bcc metals, albeit weaker [28]. Nonetheless, the Peierls barriers in these alloys appear to be stronger than those in other fcc metals. Our framework holds considerable promise in constitutive modeling in the future providing considerable insights to high entropy alloys design. In summary, our approach using multiscale resources ranging from atomistic to mesoscale, devoid of empirical constants, can help guide the work of others trying to predict stress–strain response via crystal plasticity and molecular dynamics approaches.

5. Conclusions

The work supports the following conclusions:

- The CRSS to initiate slip for the new FeNiCoCrMn high entropy alloy was determined using DIC strain measurements along a selected single crystal orientation to be $\tau_{77K} = 175$ MPa and $\tau_{293K} = 70$ MPa at 77 K and 273 K, respectively.
- Using the first principles density functional theory calculations we calculated the equilibrium lattice constant of FeNiCoCrMn as $a_0 = 3.59$ Å showing close agreement with the lattice constant $a_0 = 3.585$ Å determined using X-ray diffraction.
- Using the calculated lattice parameter a_0, the fault energy parameters γ_{us}, γ_{isf}, the shear moduli, *G*, the modified Peierls–Nabarro formalism proposed in our early work, we established the CRSS for slip to be 178 MPa which is in very close agreement with experiment ($\tau_{77K} = 175$ MPa). The remarkably close agreement between experiment and theory confirms the efficacy of our modeling framework and its potential to be applied to other high entropy alloys of significant interest.

Acknowledgments

The work was supported by Nyquist Chair Funds which is gratefully acknowledged. The authors also acknowledge the Frederick Seitz Materials Research Laboratory and Dr. Mauro Sardela for assistance with X-ray diffraction.

References

[1] J.W. Yeh, S.K. Chen, S.J. Lin, J.Y. Gan, T.S. Chin, T.T. Shun, et al., Nanostructured high-entropy alloys with multiple principal elements: novel alloy design concepts and outcomes, Adv. Eng. Mater. 6 (2004) 299–303.
[2] Y. Zhang, T.T. Zuo, Z. Tang, M.C. Gao, K.A. Dahmen, P.K. Liaw, et al., Microstructures and properties of high-entropy alloys, Prog. Mater. Sci. 61 (2014) 1–93.
[3] B. Gludovatz, A. Hohenwarter, D. Catoor, E.H. Chang, E.P. George, R.O. Ritchie, A fracture-resistant high-entropy alloy for cryogenic applications, Science 345 (2014) 1153–1158.
[4] F. Otto, A. Dlouhý, C. Somsen, H. Bei, G. Eggeler, E.P. George, The influences of temperature and microstructure on the tensile properties of a CoCrFeMnNi high-entropy alloy, Acta Mater. 61 (2013) 5743–5755.
[5] C. Zhu, Z.P. Lu, T.G. Nieh, Incipient plasticity and dislocation nucleation of FeCoCrNiMn high-entropy alloy, Acta Mater. 61 (2013) 2993–3001.
[6] J.Y. He, C. Zhu, D.Q. Zhou, W.H. Liu, T.G. Nieh, Z.P. Lu, Steady state flow of the FeCoNiCrMn high entropy alloy at elevated temperatures, Intermetallics 55 (2014) 9–14.
[7] I. Karaman, H. Sehitoglu, A.J. Beaudoin, Y.I. Chumlyakov, H.J. Maier, C.N. Tomé, Modeling the deformation behavior of Hadfield steel single and polycrystals due to twinning and slip, Acta Mater. 48 (2000) 2031.
[8] J. Carroll, W. Abuzaid, J. Lambros, H. Sehitoglu, An experimental methodology to relate local strain to microstructural texture, Rev. Sci. Instrum. 81 (2010).
[9] W.Z. Abuzaid, M.D. Sangid, J.D. Carroll, H. Sehitoglu, J. Lambros, Slip transfer and plastic strain accumulation across grain boundaries in Hastelloy X, J. Mech. Phys. Solids 60 (2012) 1201–1220.
[10] V. Vitek, Intrinsic stacking faults in body-centred cubic crystals, Philos. Mag. 18 (1968) 773–786.
[11] B. Joos, Q. Ren, M. Duesbery, Peierls–Nabarro model of dislocations in silicon with generalized stacking-fault restoring forces, Phys. Rev. B 50 (1994) 5890.
[12] G. Schoeck, The generalized Peierls–Nabarro model, Philos. Mag. A 69 (1994) 1085–1095.
[13] B. Joos, M. Duesbery, The Peierls stress of dislocations: an analytic formula, Phys. Rev. Lett. 78 (1997) 266.
[14] F. Nabarro, Theoretical and experimental estimates of the Peierls stress, Philos. Mag. A 75 (1997) 703–711.
[15] J. Wang, H. Sehitoglu, Twinning stress in shape memory alloys: theory and experiments, Acta Mater. 61 (2013) 6790–6801.
[16] A. Ojha, H. Sehitoglu, Twinning stress prediction in bcc metals and alloys, Philos. Mag. Lett. 94 (2014) 647–657.
[17] G. Kresse, J. Furthmüller, Efficiency of ab-initio total energy calculations for metals and semiconductors using a plane-wave basis set, Comput. Mater. Sci. 6 (1996) 15–50.
[18] G. Kresse, J. Furthmüller, Software VASP, vienna (1999), Phys. Rev. B 54 (1996) 169.
[19] G. Kresse, J. Hafner, Ab initio molecular dynamics for open-shell transition metals, Phys. Rev. B 48 (1993) 13115–13118.
[20] G. Kresse, J. Furthmüller, Efficient iterative schemes for ab initio total-energy calculations using a plane-wave basis set, Phys. Rev. B 54 (1996) 11169–11186.
[21] H. Suzuki, Segregation of solute atoms to stacking faults, J. Phys. Soc. Jpn. 17 (1962) 322–325.
[22] D. Finkenstadt, D.D. Johnson, Solute/defect-mediated pathway for rapid nanoprecipitation in solid solutions: γ surface analysis in fcc Al–Ag, Phys. Rev. B 73 (2006) 024101.
[23] S.A. Kibey, L.L. Wang, J.B. Liu, H.T. Johnson, H. Sehitoglu, D.D. Johnson, Quantitative prediction of twinning stress in fcc alloys: application to Cu–Al, Phys. Rev. B 79 (2009) 214202.
[24] S. Kibey, J. Liu, D. Johnson, H. Sehitoglu, Predicting twinning stress in fcc metals: linking twin-energy pathways to twin nucleation, Acta Mater. 55 (2007) 6843–6851.
[25] J. Wang, H. Sehitoglu, Modeling of pseudoelasticity via reversible slip in Fe_3Ga, Comput. Mater. Sci. 87 (2014) 34–42.
[26] A. Ojha, L. Patriarca, H. Sehitoglu, Pseudoelasticity in Fe 3 Ga with boron-A combined atomistic–micromechanical treatment, Int. J. Plast. 72 (2015) 185–199.
[27] J. Wang, H. Sehitoglu, Dislocation slip and twinning in Ni-based L1 2 type alloys, Intermetallics 52 (2014) 20–31.
[28] Z. Wu, H. Bei, G.M. Pharr, E.P. George, Temperature dependence of the mechanical properties of equiatomic solid solution alloys with face-centered cubic crystal structures, Acta Mater. 81 (2014) 428–441.

Please cite this article as: L. Patriarca, et al., Slip nucleation in single crystal FeNiCoCrMn high entropy alloy, Scripta Materialia (2015), http://dx.doi.org/10.1016/j.scriptamat.2015.09.009